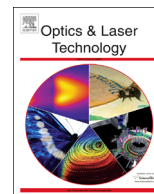




ELSEVIER

Contents lists available at ScienceDirect

Optics & Laser Technology

journal homepage: www.elsevier.com/locate/optlastec

Experimental measurement of ultrashort pulse evolution at different spatial positions in nonlinear media



Chao Tan^a, Xiquan Fu^{a,*}, Yangbao Deng^b

^a Key Laboratory for Micro-/Nano-Optoelectronic Devices of Ministry of Education, College of Information Science and Engineering, Hunan University, Changsha 410082, China

^b College of Communication and Electronic Engineering, Hunan City University, Yiyang 413002, China

ARTICLE INFO

Article history:

Received 22 August 2013

Received in revised form

13 December 2013

Accepted 14 December 2013

Available online 1 January 2014

Keywords:

Temporal evolution

Ultrashort pulse

Small-scale self-focusing

ABSTRACT

The temporal evolution of ultrashort pulses before the beam splitting is very useful for filamentation theory. In this article, we experimentally demonstrated the temporal evolution of ultrashort pulses in the different spatial positions during small-scale self-focusing. The simulation results are found to be in good agreement with experiment measurements.

© 2013 Elsevier Ltd. All rights reserved.

1. Introduction

The nonlinear propagation of ultrashort laser pulses through a Kerr medium is usually accompanied by several interesting phenomena, such as self-focusing (SF) [1], supercontinuum generation [2], multiphoton ionization [3] and filamentation [4]. SF of beam is a common phenomenon in nonlinear optics [5]. In the high power laser system, SF, especially small-scale self-focusing (SSSF), is a major factor for degradation of the laser beam quality and damage of optical materials [6,7].

When ultrashort pulses propagate in the nonlinear media, SF moves off-axis energy towards the peak of the pulse and compresses it both in spatial and temporal [8,9]. As the peak intensity increases, the process of self-phase modulation (SPM) also increases, as a result of the interplay between SPM-induced upchirp and group velocity dispersion, initiating the pulse splitting [10,11]. It is well known that Bespalov and Talanov [12] first explain the SSSF and the filamentation of a beam in terms of the modulation instability (MI) model, but they do not consider the perturbations in the temporal-domain. Campillo and Bliss et al. verify experimentally MI and the relationship among fastest growing frequency, SF length and light intensity [13–15]. The direct time-resolved observation of the propagation of intensity femtosecond laser pulses experiencing SF, beam filamentation is investigated extensively [16–19]. Previously, we have observed the evolution of spatial modulation in the process of SSSF of a beam, the

impact of relaxation effect in the media on spatial–temporal instability [20,21]. However, these studies mainly focus on the temporal evolution of the pulse in the forming and after the formation of filaments, there is little attention to the temporal evolution of the beam in the period before filamentation. Especially, the partial spatial intensity of the beam changes impact on the temporal evolution during the period of SSSF has been rarely studied. Recently, we have demonstrated the time evolution of spatial intensity increasing zones and non-increasing zones in the process of SSSF [22].

In this paper, we first demonstrate the spatial evolution of the pump beam during SSSF in the experiment and simulation. We find that there will be different growths in the different spatial positions, especially the modulation peak and modulation bottom in space, with the increase of input power. Then, we show that the temporal evolution of some spatial positions of the pump pulse monitored by a probe pulse. Due to the effect of spatiotemporal coupling, the increase of spatial intensity at modulation peak will lead to pulse width compression. However, the pulse width of modulation bottom is broadened with the increase of power, because its zone contrast is actually decreased.

2. Experiment setup

A schematic overview of our experiment setup is shown in Fig. 1. We use an amplified Ti:sapphire laser system (LibraS, Coherent, $\lambda_0 = 800$ nm) delivering pulses with bandwidth of 12 nm, single pulse energy of 1 mJ, duration $\tau_0 = 100$ fs at 1 kHz repetition rate. The beam is split into two beams by a beam splitter, BS1, one is used

* Corresponding author. Tel.: +867 318 882 4527.
E-mail address: fuxiquan@gmail.com (X. Fu).

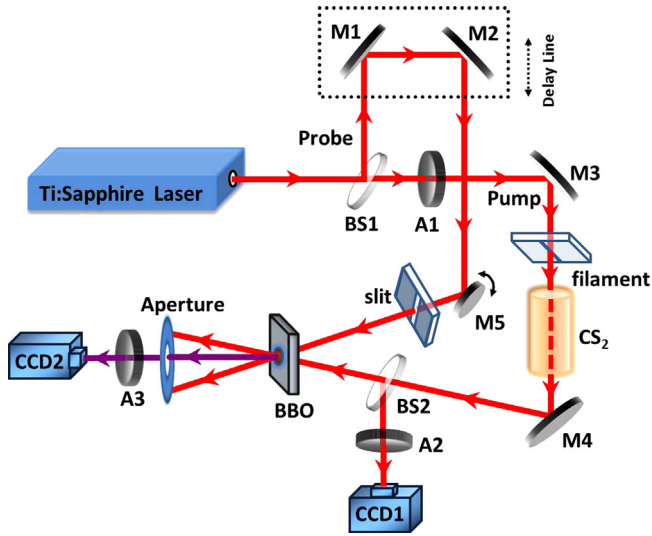


Fig. 1. Experimental setup. BS1 and BS2, beam splitters; M1 and M2, optical delay line; M3 and M4, silver-coated plane mirrors; M5, rotating mirror; A1 and A2, attenuators. (For interpretation of the references to color in this figure legend, the reader is referred to the web version of this article.)

as a pump beam and the other as a probe beam. The probe beam passes through a variable optical delay line before it is directed to a slit. A rotating mirror in front of the slit is used to change the direction of the probe beam, according that the pump beam can be scanned by the probe beam when M5 is rotated. The horizontal spatial profile of the probe beam after passing through the slit is a Sinc function distribution. The spatial and temporal scanning resolution can be controlled by adjusting the slit width and the pulse width of the probe pulse, respectively. We set the aperture of vertical slit to 0.57 mm in the experiment. A glass cuvette with 5 cm path length is filled with carbon disulfide (CS_2). CS_2 , a typical relaxing Kerr media, is chosen as the nonlinear media because of its strong Kerr nonlinearity. The pump beam is directed to the CS_2 reflected by M3. A variable attenuator, A1, is used to adjust the input power of the pump beam. A filament with diameter of 0.1 mm in front of CS_2 is used to generate initial diffraction modulation. The evolution of spatial-temporal of the pump pulse can be monitored by two synchronized high-resolution charge-coupled device (CCD) cameras (Coherent Laser Cam-HR™ Beamview, 1280×1024 pixel, pixel size of $6.7 \mu\text{m}$). In order to measure the spatial evolution of the pump beam in the front surface of BBO crystal, a part of the pump beam is imaged onto CCD1 reflected by a beam splitter, BS2. It follows that the optical path from the beam splitter, BS2, to BBO crystal is equal to from BS2 to CCD1. A sum-frequency beam generated in the BBO nonlinear crystal under noncollinear interaction of two beams is collected with a CCD2. So we can indirectly measure the temporal evolution of pump pulses by the sum-frequency beam based on the cross-correlation principle. The adjustable attenuators, A2 and A3, are custom-designed to protect CCD cameras from damage by high power laser beams.

3. Results and discussions

3.1. The spatial evolution of the beam during SSSF

Adjusting the attenuator, A1, and keeping the position of CCD1 unchanged, the spatial evolution of the pump beam which modulated by a filament in different power is shown in Fig. 2. From Fig. 2, it is easy to see distinct SSSF of the beam appears. The arrows serve to indicate the positions of the spatial modulation peak D1 and spatial modulation bottom D2. When the power is

low, the influence of nonlinear effect on the beam is far less than the diffraction effect, the diffractive modulation play a major role in the spatial evolution of the pump beam. So the SSSF at D1 is not obvious when peak power is 30.5 MW [Fig. 2(a)]. The nonlinear effect enhanced by the increment of the power and a new growth at D1 appears, the SSSF at D1 is obvious to see [Fig. 2(b), peak power ~ 90.2 MW]. When the power increased to 138.1 MW, the intensity of D1 reach maximum and a filament is formed at D1 [Fig. 2(c)]. If the power is increased continuously, the pump beam will split into multifilaments. However, the intensity of D2 not only has no significant growth with the increase of power, but its zone contrast is fall-off. Zone contrast is defined as the ratio between the partial spatial intensity and the average intensity of the beam.

Using a split-step Fourier algorithm, spatial-temporal nonlinear Schrödinger equation is used for calculation.

$$\frac{\partial A}{\partial z} = \frac{i}{2\beta_0} \left(\frac{\partial^2}{\partial x^2} + \frac{\partial^2}{\partial y^2} \right) A - \frac{i\beta_2}{2} \frac{\partial^2 A}{\partial t^2} + \frac{i\omega_0 n_2}{c} |A|^2 A$$

where A is the amplitude of the input pulse, β_0 is the transmission constant, β_2 is the group velocity dispersion, ω_0 is the central frequency, n_2 is the nonlinear index of refraction. The initial field is taken to be a Gaussian in both time and space, having an intensity full width at half maximum (FWHM) of 105 fs and 2 mm, respectively. The beam waist is located at the entrance face of the BBO. The center wavelength is $\lambda = 800$ nm, the linear index of refraction is $n_0 = 1.63$, the nonlinear index of refraction is $n_2 = 3.5 \times 10^{-15} \text{ cm}^2/\text{W}$, and the group velocity dispersion (GVD) coefficient is $\beta_2 = 1.54 \times 10^{-25} \text{ s}^2/\text{m}$. To simplify the problem, we have chosen to neglect loss and high order dispersion. The diameter of the filament is 0.1 mm and the length of nonlinear propagation is 5 cm.

The numerical simulation maps shown in Fig. 2(d)–(f) show the intensity distribution of the pump beam modulated by a filament at three different input powers. When the power is 30.5 MW, input peak power is lower than the critical power for SF, and diffractive modulation play a major role in the spatial evolution of pump beam [Fig. 2(d)]. With the increase of the power, a new growth position appears in the first modulation peak, the SSSF of beam is obvious to see [Fig. 2(e), peak power ~ 90 MW]. Because SSSF moves energy towards the modulation peak, so we can see from Fig. 2 that the intensity of modulation peak D1 increases rapidly. When the power increased to 138.1 MW, the intensity of the growth area reaches maximum [Fig. 2(f)]. However, the spatial intensity of the modulation peak cannot increase infinitely because the total energy of the beam is constant. As the power is increased continuously, new growth points will complete with the original growth point, resulting in the filamentation of the beam. No obvious growth can be observed at the modulation bottom because the SSSF effect at D2 is very weak. The simulation results are found to be in good agreement with experimental measurements.

Fig. 3(a) represents the spatial distribution of the pump beam in the horizontal plane position pointed by arrows A and B of Fig. 2(a)–(c). The numerical simulation map shown in Fig. 3(b) shows the pump beam varies with different input power. Similar to Figs. 2 and 3 displays visually the spatial evolution of laser beam modulated by a filament in the process of SSSF. With the increase of input power, nonlinear effect gradually strengthened and a new growth point in D1 appears. The intensity of D1 reach maximum when the input power increased to 138.1 MW. The intensity at D1 increased by 12% when the power is increased from 30.5 MW to 138.1 MW, the growth is a little difference between experiment and simulation at some other modulation peaks because the quality of the beam profile in the experiment is not very good. However, the zone contrast of D2 decreases with the increase of power [Fig. 3].

Download English Version:

<https://daneshyari.com/en/article/739311>

Download Persian Version:

<https://daneshyari.com/article/739311>

[Daneshyari.com](https://daneshyari.com)